Article

Cancer Cell

A Targetable GATA2-IGF2 Axis Confers Aggressiveness in Lethal Prostate Cancer

Graphical Abstract

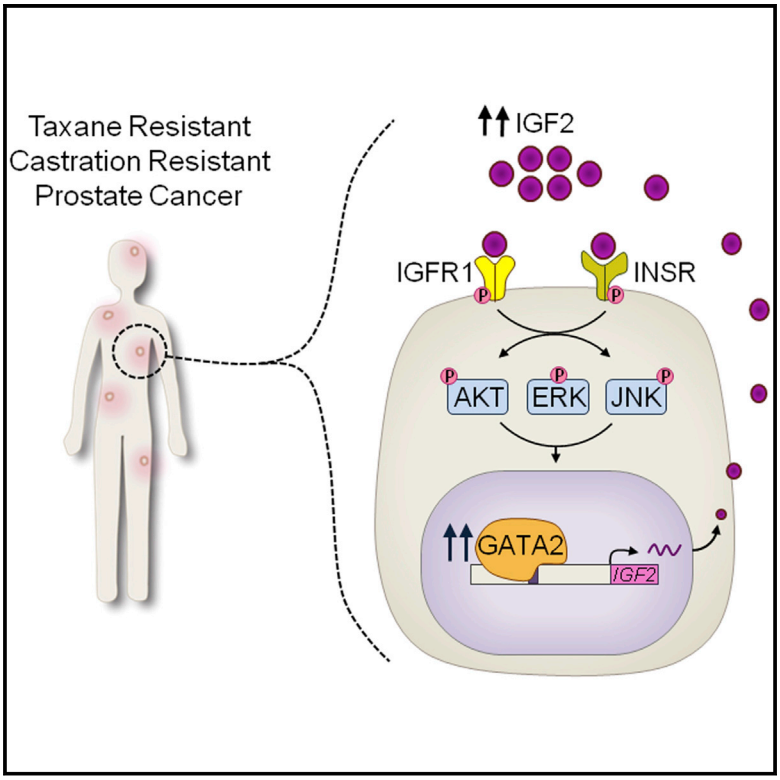

Authors

Samuel J. Vidal,
Veronica Rodriguez-Bravo, ...,
Carlos Cordon-Cardo,
Josep Domingo-Domenech

Correspondence

carlos.cordon-cardo@mssm.edu (C.C.-C.),
josep.domingo-domenech@mssm.edu (J.D.-D.)

In Brief

Vidal et al. identify GATA2 as a regulator of chemotherapy resistance and aggressiveness in prostate cancer through direct IGF2 upregulation, which stimulates IGF1R and INSR to activate downstream kinases. A dual IGF1R/INSR inhibition strategy in this context restores chemoresponsiveness.

Highlights

- GATA2 regulates chemotherapy resistance and tumorigenicity in lethal prostate cancer
- GATA2 regulates a signature of cancer-progression-associated genes that includes IGF2
- IGF2 significantly mediates the aggressive properties regulated by GATA2
- IGF1R/INSR inhibition restores the efficacy of chemotherapy and improves survival

Accession Numbers

GSE58966

Vidal et al., 2015, Cancer Cell *27*, 223–239
February 9, 2015
http://dx.doi.org/10.1016/j.ccell.2014.11.013

CellPress

Cancer Cell
Article

A Targetable GATA2-IGF2 Axis Confers Aggressiveness in Lethal Prostate Cancer

Samuel J. Vidal,[1,2] Veronica Rodriguez-Bravo,[3] S. Aidan Quinn,[4] Ruth Rodriguez-Barrueco,[2] Amaia Lujambio,[5] Estrelania Williams,[2] Xiaochen Sun,[6] Janis de la Iglesia-Vicente,[2] Albert Lee,[7] Ben Readhead,[8] Xintong Chen,[6] Matthew Galsky,[6] Berta Esteve,[2] Daniel P. Petrylak,[9] Joel T. Dudley,[8] Raul Rabadan,[7] Jose M. Silva,[2] Yujin Hoshida,[6] Scott W. Lowe,[5] Carlos Cordon-Cardo,[2,*] and Josep Domingo-Domenech[2,*]
[1]College of Physicians and Surgeons, Columbia University, New York, NY 10032, USA
[2]Department of Pathology, Icahn School of Medicine at Mount Sinai, New York, NY 10029, USA
[3]Molecular Biology Program, Memorial Sloan Kettering Cancer Center, New York, NY 10065, USA
[4]Department of Pathology and Cell Biology, Columbia University, New York, NY, USA 10032, USA
[5]Cancer Biology and Genetics Program, Memorial Sloan Kettering Cancer Center, New York, NY 10065, USA
[6]Tisch Cancer Institute, Icahn School of Medicine at Mount Sinai, New York, NY 10029, USA
[7]Department of Biomedical Informatics, Center for Computational Biology and Bioinformatics, Columbia University, New York, NY 10031, USA
[8]Department of Genetics and Genomic Sciences, Icahn School of Medicine at Mount Sinai, New York, NY 10029, USA
[9]Yale Comprehensive Cancer Center, Yale School of Medicine, New Haven, CT 06510, USA
*Correspondence: carlos.cordon-cardo@mssm.edu (C.C.-C.), josep.domingo-domenech@mssm.edu (J.D.-D.)
http://dx.doi.org/10.1016/j.ccell.2014.11.013

SUMMARY

Elucidating the determinants of aggressiveness in lethal prostate cancer may stimulate therapeutic strategies that improve clinical outcomes. We used experimental models and clinical databases to identify GATA2 as a regulator of chemotherapy resistance and tumorigenicity in this context. Mechanistically, direct upregulation of the growth hormone IGF2 emerged as a mediator of the aggressive properties regulated by GATA2. IGF2 in turn activated IGF1R and INSR as well as a downstream polykinase program. The characterization of this axis prompted a combination strategy whereby dual IGF1R/INSR inhibition restored the efficacy of chemotherapy and improved survival in preclinical models. These studies reveal a GATA2-IGF2 aggressiveness axis in lethal prostate cancer and identify a therapeutic opportunity in this challenging disease.

INTRODUCTION

Prostate cancer is a common malignancy with nearly one million annual diagnoses worldwide (Jemal et al., 2011). Among a subset of patients, primary disease eventually progresses to disseminated castration-resistant prostate cancer (CRPC). In recent years, treatment modalities that improve survival in CRPC have emerged including taxane chemotherapy (de Bono et al., 2010; Petrylak et al., 2004; Tannock et al., 2004) and second-generation androgen signaling inhibitors (Beer et al., 2014; de Bono et al., 2011; Ryan et al., 2013; Scher et al., 2012), among others. Indeed, today the first line chemotherapeutic docetaxel as well as the second line agent cabazitaxel are mainstays of treatment (Bishr and Saad, 2013). However, CRPC inexorably progresses to a chemotherapy-resistant state that ultimately precedes lethality.

GATA2 is an evolutionarily conserved zinc finger transcription factor that regulates development and differentiation in eukaryotic organisms (Vicente et al., 2012a). Mutation and deregulated expression of GATA2 are common and pathogenic in hematopoietic malignancy (Hahn et al., 2011; Vicente et al., 2012b; Zhang et al., 2008). Interestingly, GATA2 is also required for the survival of RAS-pathway-mutated non-small-cell lung cancer (NSCLC) cells (Kumar et al., 2012). In prostate cancer, GATA2 is

Significance

Disseminated castration-resistant prostate cancer (CRPC) is a common disease characterized by limited survival. However, the molecular genetics and mechanisms of therapeutic resistance in this disease remain unclear. Here we used experimental and clinical data to identify GATA2 and an associated transcriptional program as determinants of aggressiveness in this context. This approach enabled the finding that insulin-like growth factor signaling is a targetable mechanism of chemotherapy resistance and tumorigenicity downstream of GATA2. These findings shed light on the biology of lethal prostate cancer and lay the groundwork for future clinical studies.

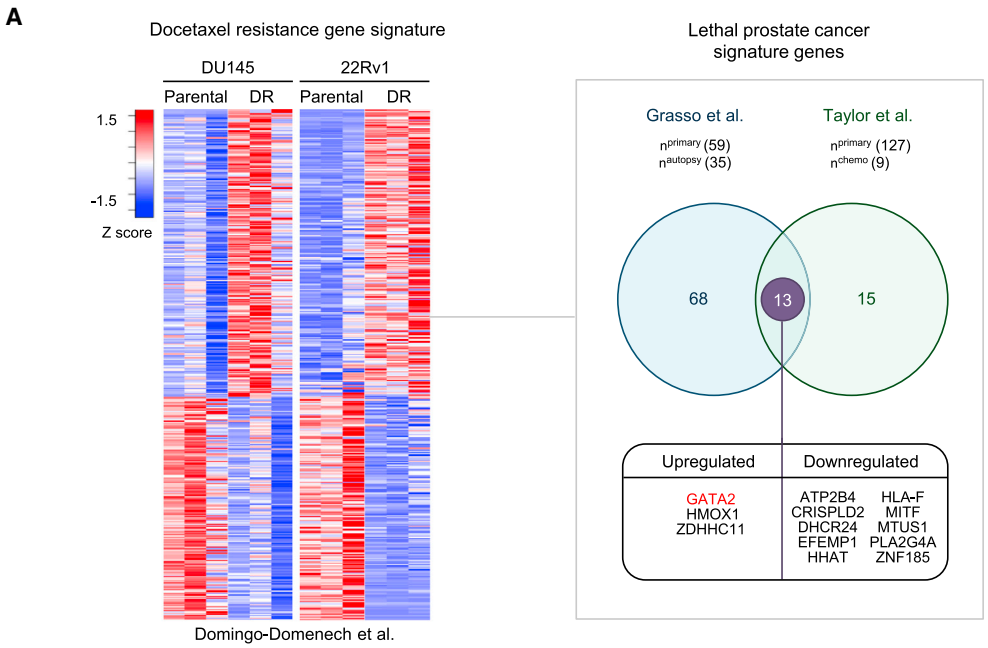

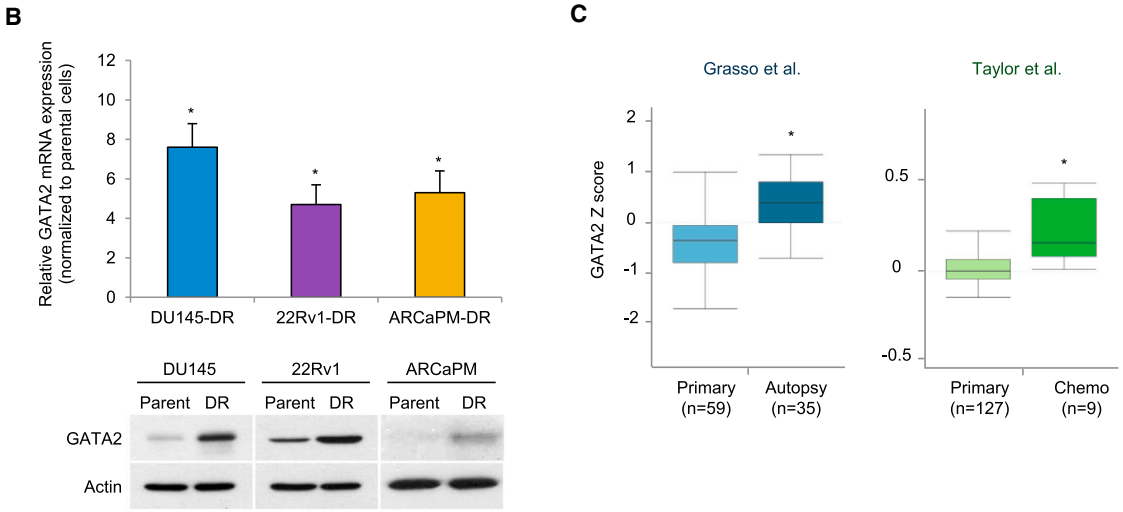

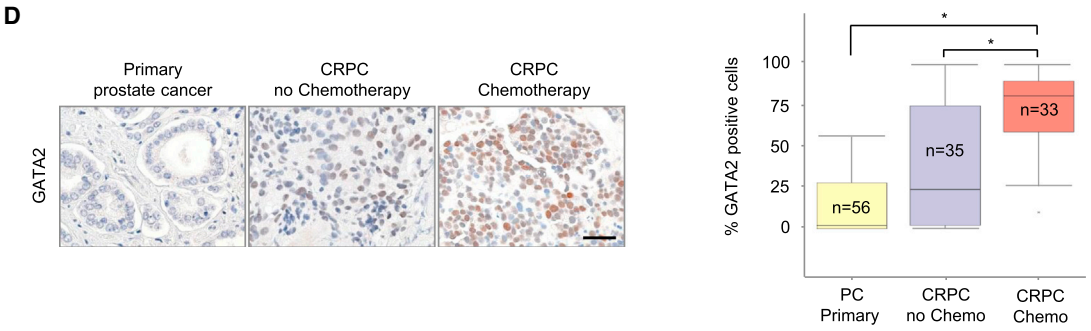

Figure 1. GATA2 Is Upregulated in Chemotherapy-Resistant Models and Lethal Prostate Cancer Tissues

(A) Venn diagram of docetaxel resistance signature genes that are differentially expressed (FDR < 0.05) during the progression from primary to lethal prostate cancer in the indicated clinical transcriptome data sets.

(legend continued on next page)

an established pioneer factor for androgen receptor (AR)-regulated genes (Chen et al., 2013; Perez-Stable et al., 2000; Wang et al., 2007; Wu et al., 2014). However, the functional attributes, downstream mechanisms, and therapeutic significance of GATA2 in prostate cancer remain unclear.

IGF2 is a growth hormone that is highly expressed during embryonic development (Stylianopoulou et al., 1988). Moreover, IGF2 is commonly overexpressed in cancer (Livingstone, 2013). Loss of imprinting is a well-described mechanism of overexpression (Feinberg and Tycko, 2004), including in early prostate cancer (Jarrard et al., 1995). In addition, IGF2 expression may be deregulated by transcription factors (Lui and Baron, 2013; Tada et al., 2014). Functionally, IGF2 overexpression is sufficient to initiate breast tumors (Bates et al., 1995; Pravtcheva and Wise, 1998) as well as several other malignancies in genetically engineered mouse models (Moorehead et al., 2003; Rogler et al., 1994). Similarly, IGF2 modulates the penetrance of large T antigen-induced islet cell tumors (Christofori et al., 1994) and PTEN-deficient breast tumors (Church et al., 2012), and IGF2 is indispensable for the formation of *Ptch*-deficient medulloblastoma and rhabdomyosarcoma (Hahn et al., 2000). Notably, while IGF2 has been associated with steroidogenesis (Lubik et al., 2013), the biology of IGF2 in prostate cancer is largely uncharacterized.

RESULTS

GATA2 Is Upregulated during the Progression to Lethal Prostate Cancer

We recently reported two models of docetaxel resistance using the CRPC cell lines DU145 and 22Rv1 (Domingo-Domenech et al., 2012). In addition to docetaxel resistance, the sublines DU145-DR and 22Rv1-DR were characterized by potent tumorigenicity and a developmental gene expression signature. To interrogate this signature for clinically relevant determinants of aggressiveness, we explored its representation in two recently published (Grasso et al., 2012; Taylor et al., 2010) data sets derived from human prostate cancer tissues. Specifically, we investigated which genes among the signature were significantly deregulated (false discovery rate [FDR] < 0.05) during the progression from primary disease to heavily treated lethal prostate cancer in the Grasso et al. (2012) study and disseminated chemotherapy-treated disease in the Taylor et al. (2010) study. We thereby identified 13 genes that were consistently deregulated in DU145-DR and 22Rv1-DR as well as during prostate cancer progression in both clinical data sets (Figure 1A). Among these candidates, GATA2 initially captured our attention as a known transcription factor and regulator of developmental biology.

We first confirmed the upregulation of GATA2 mRNA and protein in DU145-DR and 22Rv1-DR relative to their parental counterparts (Figure 1B). Moreover, we generated a third model of docetaxel resistance using the CRPC cell line ARCaPM, termed ARCaPM-DR (Figures S1A and S1B available online). Notably, ARCaPM-DR exhibited increased tumorigenicity (Figure S1C) as well as increased levels of GATA2 mRNA and protein (Figure 1B). Interestingly, all three models of docetaxel resistance exhibited varying degrees of cross-resistance to cabazitaxel (Figures S1D–S1G), suggesting that the molecular landscape of the docetaxel-resistant models also confers resistance to this second line taxane. Finally, we confirmed upregulation of GATA2 mRNA during disease progression in the two clinical data sets (Figure 1C).

To further characterize the expression of GATA2 in clinical prostate cancer, we performed an immunohistochemistry analysis in a series of 124 paraffin-embedded tissues. We observed that GATA2 protein levels increased during the progression from primary prostate cancer to disseminated CRPC, while the subset of patients treated with taxane chemotherapy exhibited the highest levels (Figure 1D).

GATA2 Regulates Chemotherapy Resistance and Tumorigenicity

Our data supported a possible association between GATA2, chemotherapy resistance, and tumorigenicity in CRPC. To further investigate this association, we characterized two short hairpin RNAs (shRNAs) that efficiently reduced the mRNA and protein levels of GATA2 in the three chemotherapy-resistant cultures (Figure 2A). Colony-formation assays revealed that GATA2 knockdown sensitized the three cultures to docetaxel and cabazitaxel (Figure 2B), and further experiments showed that sensitization was accompanied by increased induction of apoptosis (Figures 2C and 2D). In addition, xenotransplantation studies showed that GATA2 knockdown reduced the capacity of CRPC cells to form tumors in vivo (Figure S2A). For example, following implantation of 100 cells, GATA2 knockdown completely abrogated the tumorigenicity of the chemotherapy-resistant cultures (Figure 2E). Moreover, while infrequent tumors formed at larger inoculums, they did so after long latencies and likely as a result of escape from GATA2 knockdown (Figure S2B).

To extend these findings to patient-derived xenograft models, we collected circulating tumor cells from CRPC patients with chemotherapy-resistant disease. We stably propagated two xenografts termed lethal prostate cancer 1 (LPC1) and lethal prostate cancer 2 (LPC2) in mice, and characterized their human prostate cancer origin and genomic stability over serial passages (Figures S2C–S2F). We also confirmed their castration- and taxane-resistant properties in vivo (Figures S2G and S2H). Moreover, we developed an intratumoral small interfering RNA (siRNA) protocol that enabled consistent GATA2 mRNA and protein suppression in subcutaneous tumors (Figure S2I). We first combined this protocol with a vehicle, docetaxel, or cabazitaxel regimen over a period of 4 weeks. Tumor volume (Figure 2F) and

(B) Quantitative RT-PCR (qRT-PCR) and immunoblot analyses of GATA2 mRNA and protein levels, respectively, in DU145-DR, 22Rv1-DR, and ARCaPM-DR cells relative to their parental cell lines. Data represent the mean ± SD. *$p < 0.05$.

(C) Box plots of GATA2 mRNA levels during disease progression in the indicated clinical transcriptome data sets. Line, median; box, 25th to 75th percentiles; bars, 1.5 times interquartile range (IQR); dots, outliers. *$p < 0.05$.

(D) Representative immunohistochemistry images and quantifications of GATA2 protein levels during disease progression in a series of human paraffin-embedded prostate cancer tissues. Line, median; box, 25th to 75th percentiles; bars, 1.5 times IQR; dots, outliers. n = 124. Scale bar, 100 μm. *$p < 0.05$.

See also Figure S1.

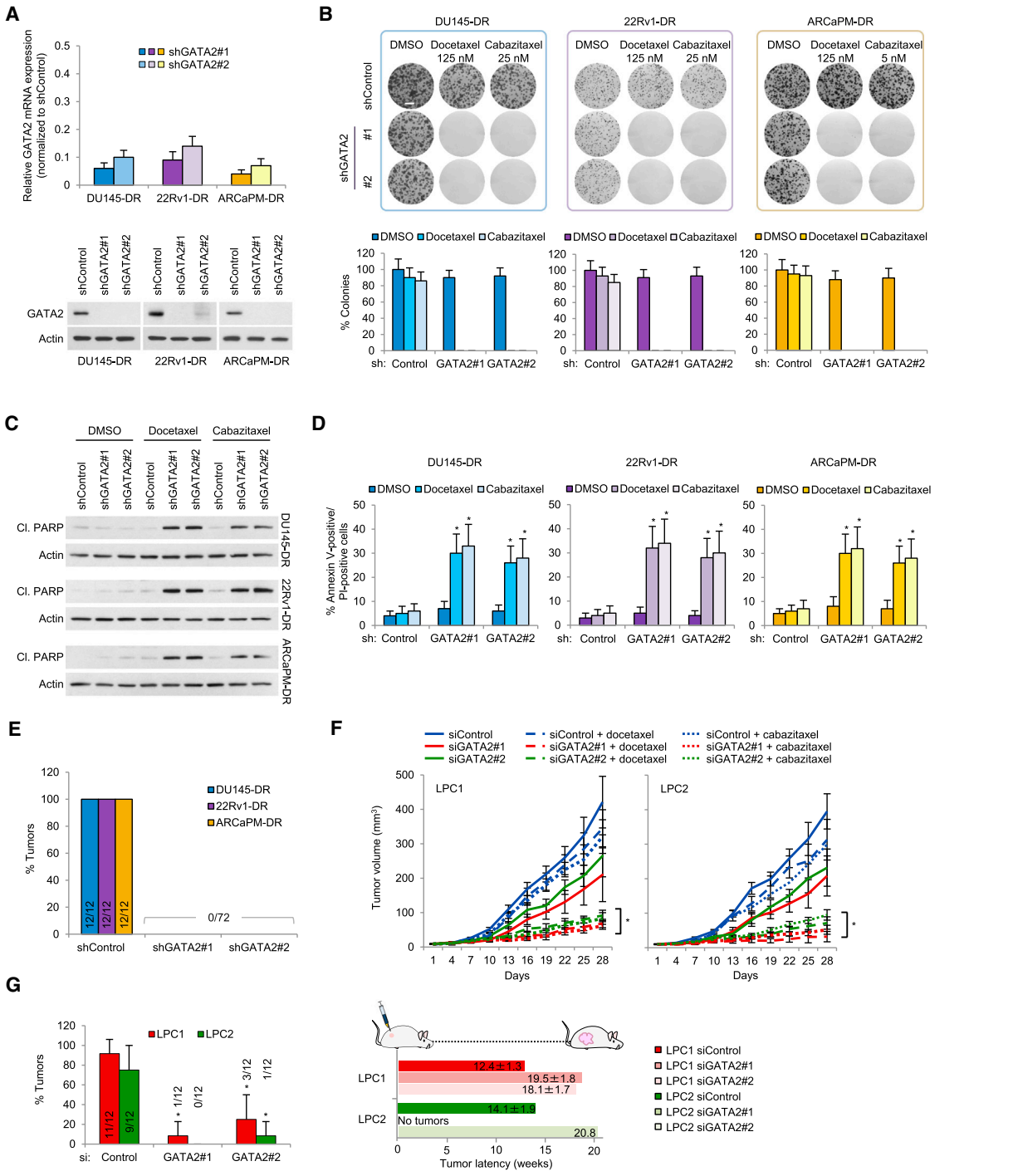

Figure 2. GATA2 Regulates Chemotherapy Resistance and Tumorigenicity in CRPC

(A) qRT-PCR and immunoblot analyses of GATA2 mRNA and protein levels, respectively, in DU145-DR, 22Rv1-DR, and ARCaPM-DR cells stably expressing two independent GATA2 shRNAs or a control shRNA. Data represent the mean ± SD.

(B) Representative colony-formation assays and quantifications of DU145-DR, 22Rv1-DR, and ARCaPM-DR cells stably expressing indicated control or GATA2 shRNAs and following 72 hr treatment with DMSO, docetaxel (125 nM), or cabazitaxel (DU145-DR and 22Rv1-DR, 25 nM; ARCaPM-DR, 5 nM). Scale bar, 100 μm. Data represent the mean ± SD.

(C) Immunoblots of cleaved (Cl.) PARP levels in the same cells and following the same treatments described in (B).

(D) Flow cytometry detection of Annexin V and PI in the same cells and following the same treatments described in (B). Data represent the mean ± SD. *$p < 0.05$.

(E) Tumorigenicity of DU145-DR, 22Rv1-DR, and ARCaPM-DR cells stably expressing indicated control or GATA2 shRNAs.

(legend continued on next page)

weight (Figure S2J) measurements showed that GATA2 regulated chemotherapy resistance in the LPC models. In addition, we serially transplanted xenograft cells following 2 weeks of siRNA treatment without chemotherapy. These studies showed that GATA2 suppression caused LPC1 and LPC2 cells to form tumors with reduced incidence and increased latency in secondary recipients (Figures 2G and S2K). Therefore, our data collectively suggest that GATA2 confers aggressiveness in CRPC by regulating chemotherapy resistance and tumorigenicity.

GATA2 Regulates a Signature of Cancer-Progression-Associated Genes

To elucidate mechanisms whereby GATA2 regulates these properties, we performed expression profiling and knowledge-based computational studies comparing control and GATA2 knockdown conditions. Prompted by the observation that GATA2 regulates similar properties in DU145-DR, 22Rv1-DR, and ARCaPM-DR, we focused an initial series of studies on mechanisms overlapping among the three models. RNA sequencing followed by differential expression analysis ($P_{adj} < 0.05$, fold change [FC] ≥ 1.5) resulted in the identification of a consensus 28-member signature of GATA2-regulated genes (Figures 3A and 3B). In addition, gene ontology analysis showed that (1) cancer, (2) cell death and survival, and (3) cellular growth and proliferation were the most commonly deregulated biological categories (Figure 3C). To assess the clinical relevance of the consensus signature, we performed Pearson correlation coefficient calculations comparing the average expression of the signature and the expression data of patients, as previously described (Liu et al., 2007). These calculations revealed that the 28-gene signature was remarkably enriched in the lethal prostate cancer population from the large Grasso et al. (2012) study (Figure 3D). Similarly, the signature was significantly enriched in the disseminated chemotherapy-treated population from the Taylor et al. (2010) study (Figure 3D).

To further distill the consensus signature to its clinically salient components, we focused on genes that exhibited the most robust differential expression pattern consistent with regulation by GATA2 in patient-derived data sets. We thereby identified a core subset of seven genes that demonstrated both uniform deregulation by GATA2 knockdown in the three chemotherapy-resistant cultures (Figure 3E) as well as complementary (FDR < 0.1) expression patterns during disease progression in the Grasso et al. (2012) and Taylor et al. (2010) studies (Figure 3F). Interestingly, all seven genes exhibited corresponding expression patterns in the chemotherapy-resistant cultures relative to their parental counterparts (Figure S3A), suggesting possible roles in chemotherapy resistance, tumorigenicity, or both. To functionally characterize these genes, we performed RNA interference (genes repressed by GATA2 knockdown) and overexpression (genes derepressed by GATA2 knockdown) studies using the three chemotherapy-resistant cultures (Figure S3B). We monitored both chemotherapy resistance and soft agar growth as a surrogate for in vivo tumorigenicity. Notably, five of the seven genes consistently regulated chemotherapy resistance (Figure 3G), soft agar growth (Figure 3H), or both. These results suggest that GATA2 regulates a discrete network of clinically and biologically significant genes during the progression to lethal prostate cancer.

Finally, mindful of previous reports establishing GATA2 as a pioneer factor for AR-regulated genes, we focused a second series of studies on this association. Consistent with their parental lines, DU145-DR and ARCaPM-DR lacked AR protein (Figure S3C), indicating that AR is dispensable for regulation of the consensus 28-gene signature by GATA2. This observation was further supported by the near complete failure of the 28-gene signature to overlap with more than one thousand known AR-regulated genes from two published (Sharma et al., 2013; Wang et al., 2009) CRPC studies (Figure S3D). Moreover, the core GATA2-regulated genes identified in our studies were unresponsive to AR knockdown in the AR-expressing 22Rv1-DR culture (Figure S3E). Therefore, our data suggest that the consensus GATA2 signature is unrelated to AR biology. Nonetheless, we observed that subsets of AR-regulated genes from the Sharma et al. (2013) and Wang et al. (2009) studies were significantly deregulated by GATA2 knockdown in the AR-expressing 22Rv1-DR culture (Figure S3F). Notably, these GATA2- and AR-regulated genes included the canonical AR targets KLK3 and TMPRSS2 (Figure S3G), corroborating previous reports (Perez-Stable et al., 2000; Wang et al., 2007) that GATA2 functions as a pioneer factor for AR at these loci. However, the GATA2- and AR-regulated signatures were not consistently deregulated in 22Rv1-DR relative to its parental line (Figure S3H), suggesting that they do not contribute to chemotherapy resistance or tumorigenicity. Complementing this hypothesis, the GATA2- and AR-regulated signatures were poorly correlated with progression to chemotherapy-treated disease in clinical data sets (Figure S3I). Therefore, our data collectively suggest that, in addition to its established pioneer function at AR-regulated sites, GATA2 regulates clinically relevant AR-independent genes (Figure 3B) that confer chemotherapy-resistant and tumorigenic properties in lethal prostate cancer.

Direct Upregulation of IGF2 Contributes to the Aggressive Properties Regulated by GATA2

We next investigated whether GATA2 regulates actionable targets with the potential to confer therapeutic benefit. Among the functionally validated GATA2-regulated genes (Figures 3G and 3H), IGF2 was distinctive through its strong and consistent regulation of both chemotherapy resistance and soft agar growth. Indeed, as a canonical activator of insulin-like growth factor signaling, IGF2 promotes aggressive properties in a multitude of malignancies (Livingstone, 2013). In addition, we noted that several insulin-like growth factor pathway inhibitors are

(F) Volumes of LPC1 and LPC2 subcutaneous xenografts during 28 days of combination treatment with vehicle, docetaxel (10 mg/kg i.p. weekly), or cabazitaxel (10 mg/kg i.p. weekly) as well as indicated control or GATA2 intratumoral siRNAs. Data represent the mean ± SD. *$p < 0.05$.

(G) Tumor incidence and latency of LPC1 and LPC2 cells following 14 days of treatment with indicated intratumoral siRNAs. Data represent the mean ± SD. *$p < 0.05$.

See also Figure S2.

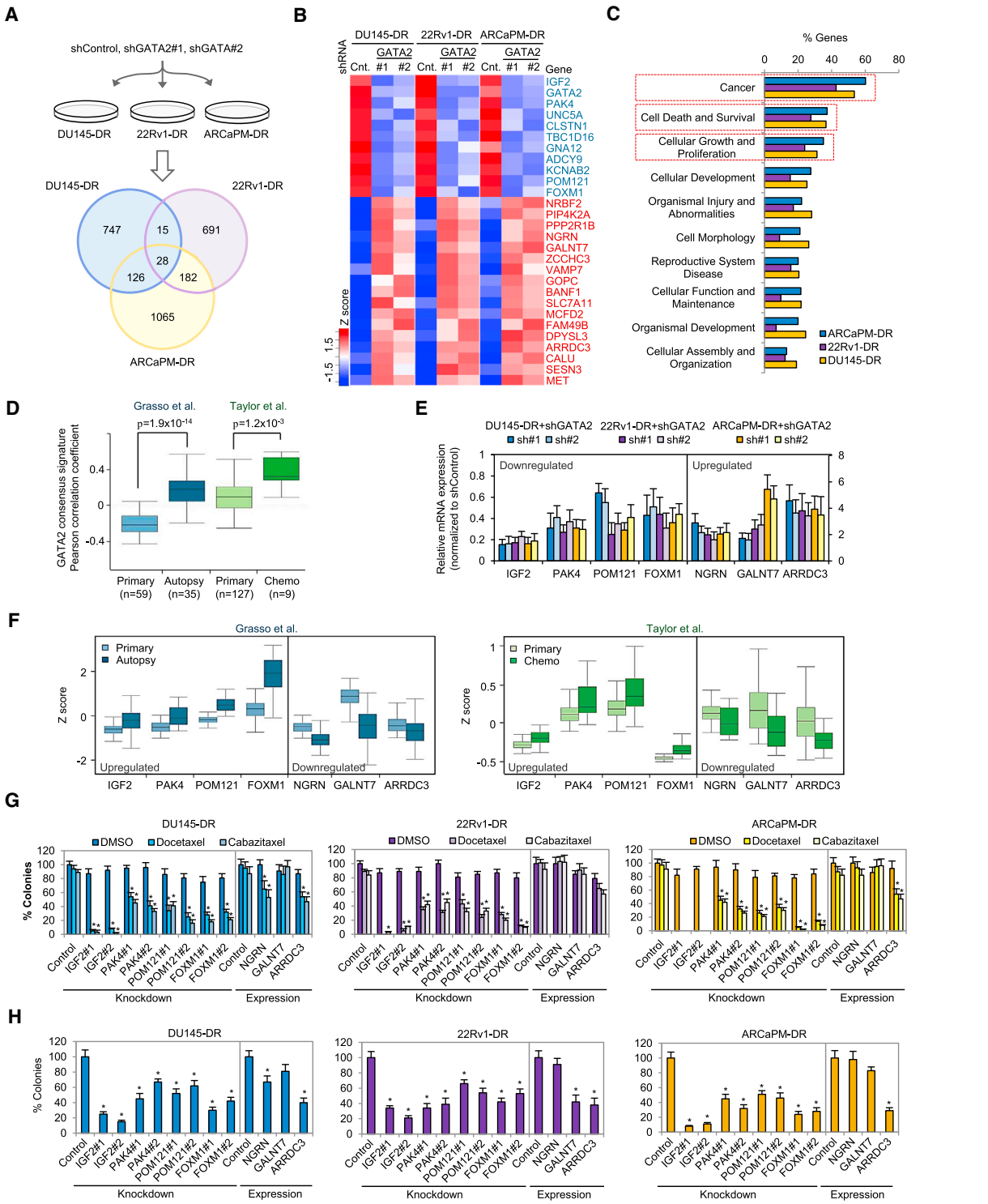

Figure 3. GATA2 Regulates a Signature of Cancer-Progression-Associated Genes

(A) Venn diagram of differentially expressed genes (p_{adj} < 0.05 and FC ≥ 1.5) identified by RNA sequencing after shRNA-mediated GATA2 knockdown in DU145-DR, 22Rv1-DR, and ARCaPM-DR cells.

(B) Heatmap of the consensus 28-member signature of GATA2-regulated genes from (A).

(C) Ingenuity knowledge-based molecular and cellular functions analysis of GATA2-regulated genes in DU145-DR, 22Rv1-DR, and ARCaPM-DR cells from (A).

(D) Box plots of the Pearson coefficients for the correlation between the expression data of each patient in the indicated clinical transcriptome data sets and the average expression of the GATA2 gene signature from (A) during prostate cancer progression. Line, median; box, 25th to 75th percentiles; bars, 1.5 times IQR; dots, outliers.

(legend continued on next page)

currently in advanced clinical development. Together, these observations credentialed IGF2 as a biologically and therapeutically meritorious candidate downstream of GATA2, and we therefore selected it for more detailed analysis.

We performed a series of studies to clearly establish IGF2 as a functional mediator of GATA2 biology. First, two independent shRNAs efficiently reduced the mRNA and protein levels of IGF2 in the three chemotherapy-resistant cultures (Figure S4A). Colony-formation (Figure 4A) and xenotransplantation (Figure 4B) studies showed that IGF2 knockdown reduced the chemotherapy-resistant and tumorigenic properties of these cells, respectively. Moreover, IGF2 was abundantly secreted into the medium of the chemotherapy-resistant cultures (Figure S4B), and addition of a neutralizing anti-IGF2 immunoglobulin reduced their taxane resistance (Figure 4C) and soft agar growth (Figure 4D). Next, we transduced control and GATA2 knockdown cells with a control or IGF2 expression vector (Figure S4C). Notably, colony-formation (Figure 4E) and xenotransplantation (Figure 4F) studies showed that IGF2 expression significantly rescued the biological defects instigated by GATA2 knockdown in the chemotherapy-resistant cultures. Moreover, addition of recombinant IGF2 to the medium of the chemotherapy-resistant cultures rescued the defects instigated by GATA2 on taxane resistance (Figure S4D) and soft agar growth (Figure S4E). Collectively, these results suggest that IGF2 substantially mediates the chemotherapy-resistant and tumorigenic properties of CRPC cells downstream of GATA2.

We previously observed that IGF2 mRNA levels are strongly upregulated (Figure S3A) and responsive to GATA2 knockdown (Figure 3E) in the three chemotherapy-resistant cultures. We first confirmed these observations at the protein level (Figures 5A and 5B). In addition, GATA2 overexpression (Figure S5A) in the parental cell lines increased their taxane resistance (Figures S5B and S5C) and tumorigenicity (Figure S5D) as well as the mRNA (Figure 5C) and protein (Figure 5D) levels of IGF2. Therefore, we next investigated the mechanism whereby GATA2 regulates IGF2 expression. The human IGF2 gene is transcribed from at least four promoters termed P1 through P4 (Livingstone, 2013). Interestingly, probing the TRANSFAC database with these promoter sequences indicated that P4 contains two predicted GATA2-binding elements (GBEs), which we termed GBE1 and GBE2 (Figure S5E). Indeed, chromatin immunoprecipitation followed by qPCR (ChIP-qPCR) studies revealed that GATA2 occupies the GBEs in the three chemotherapy-resistant cultures but not adjacent control regions (Figure 5E). In addition, cotransfection assays showed that GATA2 expression could activate luciferase transcription from a P4 reporter in the three parental cell lines, while mutation of the GBEs reversed this effect (Figure 5F). Moreover, these observations were independently validated in embryonic fibroblast cells (Figure 5G). Thus, we observed that GATA2 may occupy predicted binding elements in the P4 sequence and thereby activate IGF2 transcription.

Finally, a corollary of our hypothesis that GATA2 transcriptionally upregulates IGF2 is that these genes are coexpressed in clinical prostate cancer tissues. Indeed, we previously observed that IGF2 is upregulated during disease progression in the Grasso et al. (2012) and Taylor et al. (2010) studies (Figure 3E). To confirm and extend this finding, we performed an immunohistochemistry analysis with our cohort of human paraffin-embedded prostate cancer tissues. We observed that IGF2 protein expression increases during the progression from primary prostate cancer to disseminated CRPC, while the subset of patients treated with taxane chemotherapy exhibited the highest levels (Figure 5H). Moreover, among a subset of disseminated CRPC tissues without previous chemotherapy, levels of both GATA2 and IGF2 were associated with response to subsequent docetaxel treatment (Figure S5F).

IGF2 Activates a Polykinase Program Downstream of GATA2

We next investigated possible downstream mechanisms underlying the GATA2-IGF2 axis. IGF2 exhibits homology with insulin, and IGF2 ligand binding may activate both the insulin-like growth factor 1 receptor (IGF1R) and insulin receptor (INSR) tyrosine kinases (Livingstone, 2013). The receptors phosphorylate scaffolding intermediates including IRS and SHC, which, in turn, activate phosphoinositide 3 kinase (PI3K) and mitogen-activated protein kinase (MAPK) signaling, respectively. Accordingly, the downstream effectors of insulin-like growth factor pathway signaling principally include AKT, JNK, ERK1/2, and p38 and are context dependent.

Immunoprecipitation studies revealed that IGF2 knockdown in the chemotherapy-resistant cultures resulted in dephosphorylation of both the IGF1R and INSR tyrosine kinases (Figure 6A). We also noted dephosphorylation of both IRS and SHC scaffolding intermediaries, suggesting that IGF2 may activate both the PI3K and MAPK pathways, respectively (Figure 6B). Indeed, further studies revealed that IGF2 knockdown consistently resulted in dephosphorylation of AKT and JNK, but not p38, in the three chemotherapy-resistant cultures. In addition, ERK1/2 was dephosphorylated in DU145-DR, but not 22Rv1-DR or ARCaPM-DR. Concordantly, this kinase phosphorylation pattern was specifically increased in the chemotherapy-resistant cultures relative to their parental counterparts (Figure S6A). Moreover, GATA2 knockdown in the chemotherapy-resistant cell lines also recapitulated the phosphorylation pattern, while an IGF2 expression vector resulted in a complete rescue (Figure 6C).

(E) qRT-PCR of mRNA levels of a subset of cancer-progression-associated genes in DU145-DR, 22Rv1-DR, and ARCaPM-DR cells stably expressing indicated control or GATA2 shRNAs. Data represent the mean ± SD.

(F) Z scores of mRNA levels of genes from (D) in the indicated clinical transcriptome data sets. Line, median; box, 25th to 75th percentiles; bars, 1.5 times IQR.

(G) Colony-formation assay quantifications of DU145-DR, 22Rv1-DR, and ARCaPM-DR cells transfected with indicated siRNAs or stable expression vectors and following 72 hr treatment with DMSO, docetaxel (125 nM), or cabazitaxel (DU145-DR and 22Rv1-DR, 25 nM; ARCaPM-DR, 5 nM). Data represent the mean ± SD. *$p < 0.05$.

(H) Soft agar colony-formation assay quantifications of DU145-DR, 22Rv1-DR, and ARCaPM-DR transfected with indicated siRNAs or stable expression vectors. Data represent the mean ± SD. *$p < 0.05$.

See also Figure S3.

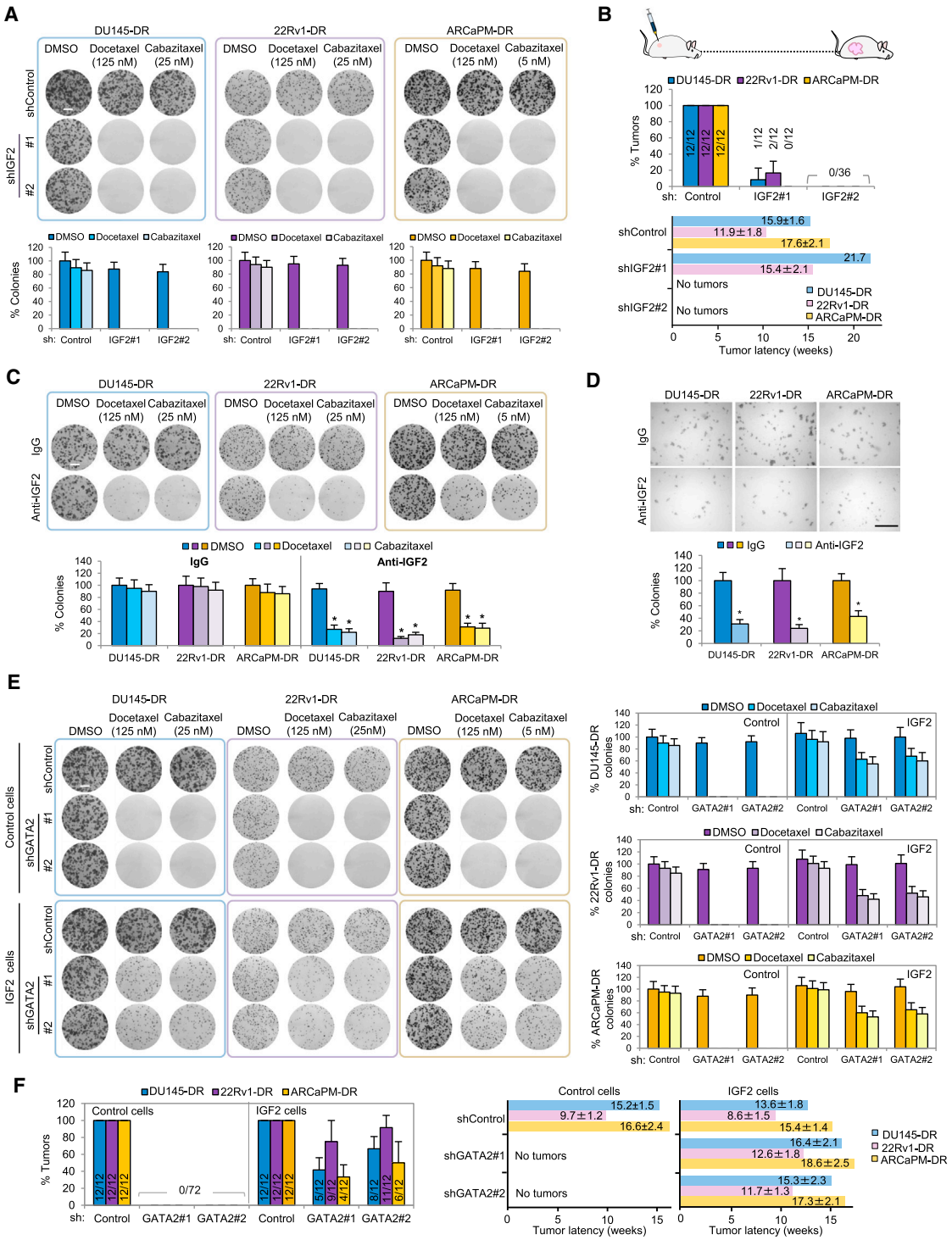

Figure 4. IGF2 Contributes to the Aggressive Properties Regulated by GATA2

(A) Representative colony-formation assays and quantifications of DU145-DR, 22Rv1-DR, and ARCaPM-DR cells stably expressing indicated control or IGF2 shRNAs and following 72 hr treatment with DMSO, docetaxel, or cabazitaxel. Scale bar, 100 μm. Data represent the mean ± SD.

(B) Tumor incidence and latency of DU145-DR, 22Rv1-DR, and ARCaPM-DR cells stably expressing indicated control or IGF2 shRNAs. Data represent the mean ± SD. *$p < 0.05$.

(C) Representative colony-formation assays and quantifications of DU145-DR, 22Rv1-DR, and ARCaPM-DR cells following 72 hr treatment with isotype control or anti-IGF2 immunoglobulin (10 μg/ml) as well as DMSO, docetaxel, or cabazitaxel. Scale bar, 100 μm. Data represent the mean ± SD. *$p < 0.05$.

(D) Representative soft agar colony-formation assays and quantifications of DU145-DR, 22Rv1-DR, and ARCaPM-DR cells treated continuously with isotype control or anti-IGF2 immunoglobulin (10 μg/ml). Scale bar, 100 μm. Data represent the mean ± SD. *$p < 0.05$.

(legend continued on next page)

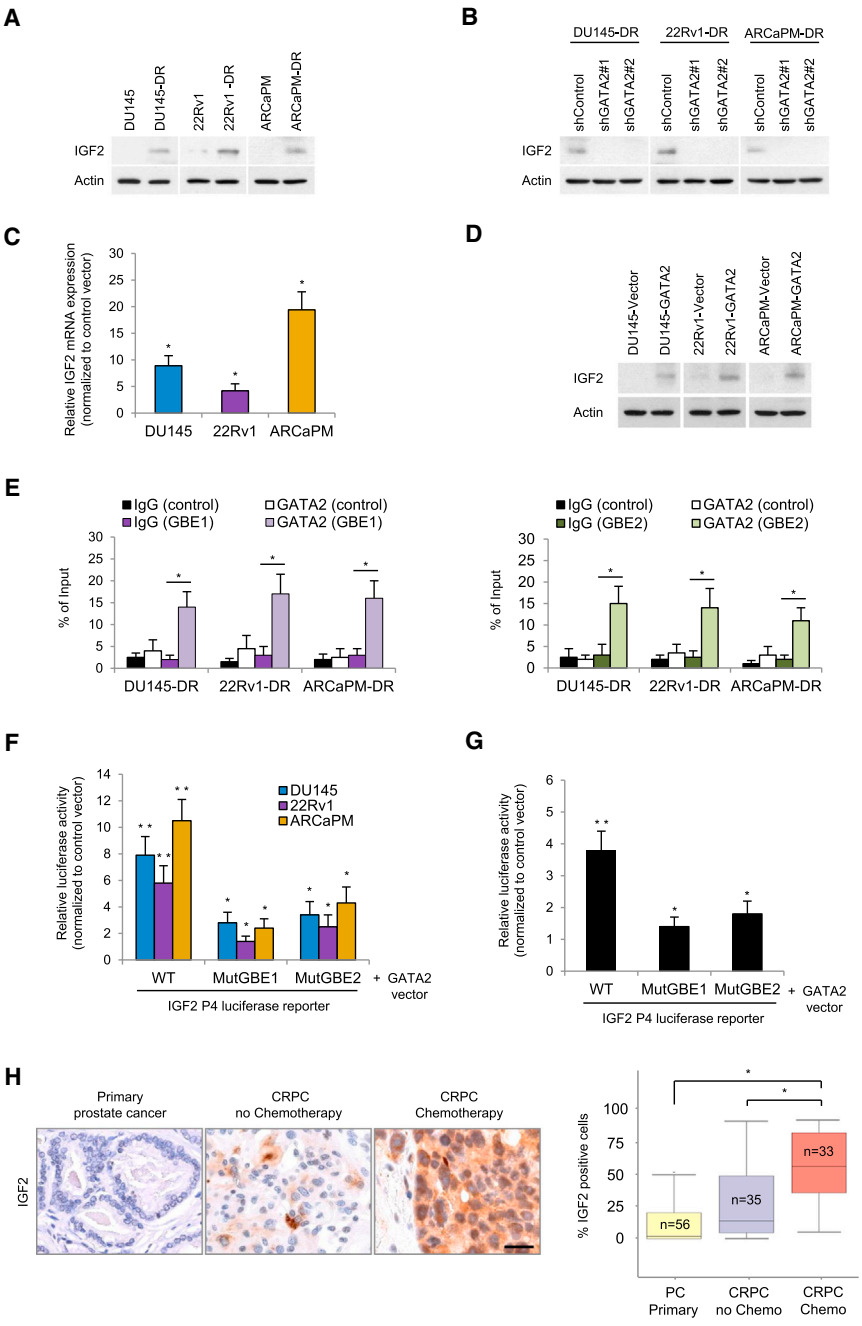

Figure 5. GATA2 Directly Regulates IGF2 Expression

(A) Immunoblots of IGF2 protein levels in DU145-DR, 22Rv1-DR, and ARCaPM-DR cells relative to their parental cell lines.

(B) Immunoblots of IGF2 protein levels in DU145-DR, 22Rv1-DR, and ARCaPM-DR cells stably expressing indicated control or GATA2 shRNAs.

(C) qRT-PCR of IGF2 mRNA levels in DU145, 22Rv1, and ARCaPM cells stably expressing a control or GATA2 expression vector. Data represent the mean ± SD. *$p < 0.05$.

(D) Immunoblots of IGF2 protein levels in cells from (C).

(E) ChIP-qPCR of GATA2 occupancy at GBE1, GBE2, and flanking control regions in DU145-DR, 22Rv1-DR, and ARCaPM-DR cells. Data represent the mean ± SD. *$p < 0.05$.

(F) Luciferase luminescence of parental CRPC cells following cotransfection with a control or GATA2 expression vector, a P4 luciferase reporter (wild-type [WT], mutated GBE1 [mutGBE1], or mutated GBE2 [mutGBE2]), and a renilla transfection efficiency control. Data represent the mean ± SD. *$p < 0.05$. **$p < 0.05$ relative to control vector.

(G) Luciferase luminescence of NIH 3T3 cells following same experimental conditions as in (F). Data represent the mean ± SD. *$p < 0.05$. **$p < 0.05$ relative to control vector.

(H) Representative immunohistochemistry images and quantifications of IGF2 protein levels during disease progression in a series of human paraffin-embedded prostate cancer tissues. Line, median; box, 25th to 75th percentiles; bars, 1.5 times IQR; dots, outliers. n = 124. Scale bar, 100 μm. *$p < 0.05$. See also Figure S5.

These results suggested that GATA2 regulates a context-dependent polykinase program through upregulation of IGF2. Indeed, GATA2 suppression in the LPC xenografts (Figure S2H) resulted in reduced IGF2 protein levels as well as dephosphorylation of AKT, JNK, and ERK1/2 in a context-dependent manner (Figure S6B), and IGF2 suppression yielded similar results (Figure S6C).

We next examined whether the polykinase program regulated by GATA2 and IGF2 is functionally significant. To this end, we evaluated the effect of two independent combinations of well-characterized chemical inhibitors of PI3K/AKT (LY294002 and MK2206), JNK (SP600125 and AS601245), and MEK (U0126 and PD98059) on chemotherapy resistance and soft agar growth as a surrogate for tumorigenicity in our three in vitro models. We observed that combined inhibition of PI3K/AKT and JNK signaling strongly diminished the chemotherapy resistance (Figures 6D and S6D) and soft agar growth (Figures 6E and S6E) of the three models. Moreover, as predicted by our immunoblot results (Figures 6B and 6C), MEK/ERK signaling

(E) Representative colony-formation assays and quantifications of DU145-DR, 22Rv1-DR, and ARCaPM-DR cells stably expressing indicated control or GATA2 shRNAs as well as a control or IGF2 expression vector and following 72 hr treatment with DMSO, docetaxel, or cabazitaxel. Scale bar, 100 μm. Data represent the mean ± SD.

(F) Tumor incidence and latency of DU145-DR, 22Rv1-DR, and ARCaPM-DR cells stably expressing indicated control or GATA2 shRNAs as well as a control or IGF2 expression vector. Data represent the mean ± SD.

See also Figure S4.

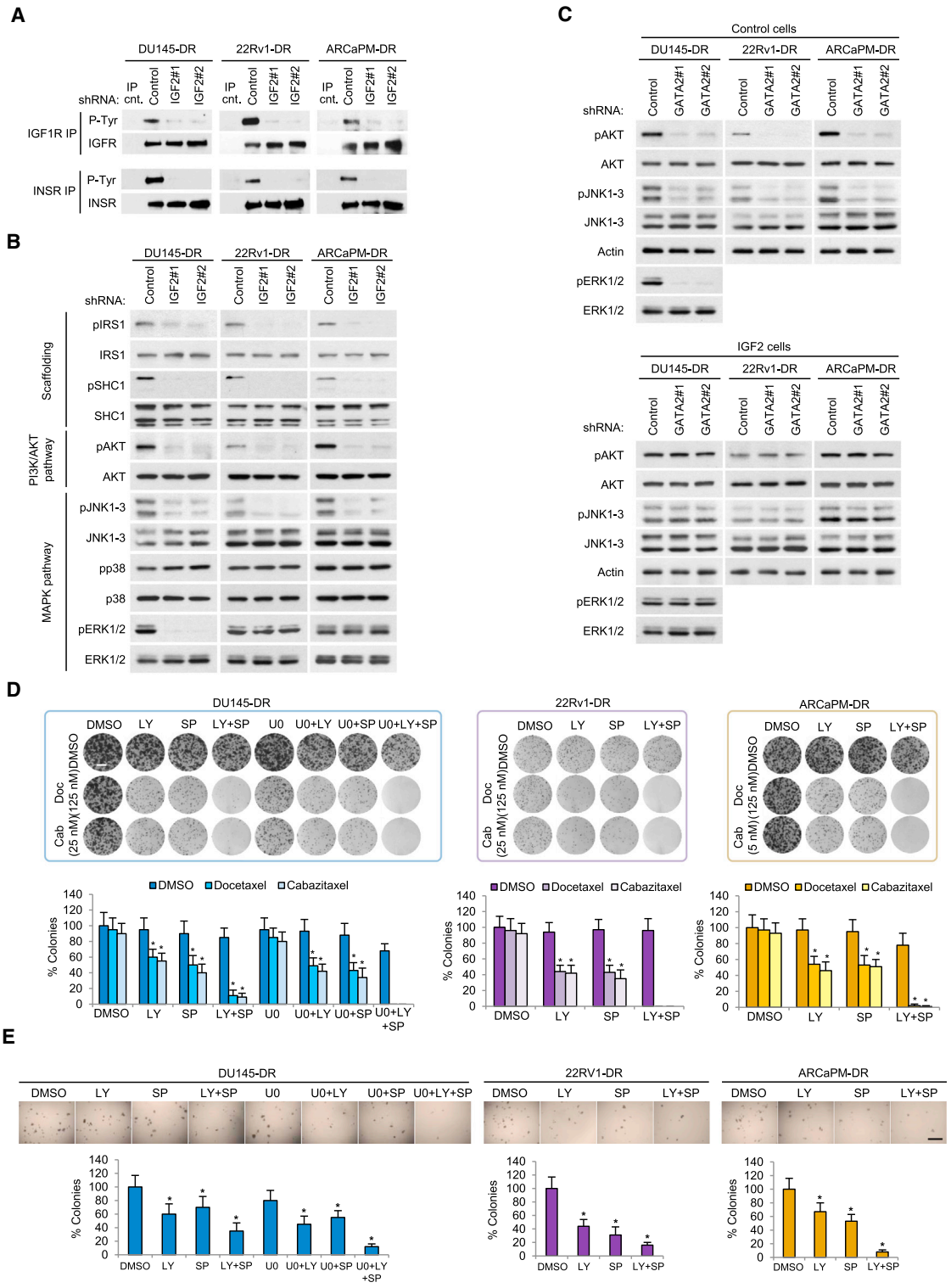

Figure 6. IGF2 Activates a Polykinase Program Downstream of GATA2 that Regulates Chemotherapy Resistance and Soft Agar Growth

(A) Immunoblots of phospho-tyrosine (pTyr) levels following immunoprecipitation of IGF1R or INSR in DU145-DR, 22Rv1-DR, and ARCaPM-DR cells stably expressing two independent IGF2 shRNAs or a control shRNA in serum-free conditions.

(B) Immunoblots of relevant insulin-like growth factor signaling protein levels in DU145-DR, 22Rv1-DR, and ARCaPM-DR cells stably expressing indicated control or IGF2 shRNAs in serum-free conditions.

(legend continued on next page)

inhibition in the DU145-DR model further attenuated these properties. Therefore, our data collectively suggest that GATA2 confers aggressive properties in part through a network of kinases downstream of IGF2.

Insulin-like growth factor signaling is known to broadly confer survival properties through PI3K/AKT and MAPK signaling (Vincent and Feldman, 2002). Interestingly, we observed that increased expression of IGF2 (Figures S3A and 5A) and activation of the polykinase program (Figure S6A) in the chemotherapy-resistant cultures were associated with increased resistance to additional apoptotic stimuli. For example, exposure of the chemotherapy-resistant cultures to both radiation and oxidative stress resulted in reduced levels of apoptosis relative to their parental counterparts (Figure S6F). Moreover, these observations were reverted upon IGF2 knockdown (Figure S6G), suggesting that insulin-like growth factor signaling confers broad survival properties in our chemotherapy-resistant models.

Finally, we explored the relationship between the GATA2-IGF2 axis in our chemotherapy-resistant models and our previous report of Notch- and Hedgehog-dependent tumor-initiating cells (T-ICs) in the parental cell lines (Domingo-Domenech et al., 2012). Following both GATA2 knockdown in the chemotherapy-resistant sublines (Figures S7A and S7B) and overexpression in the parental cell lines (Figures S7C and S7D), we observed no effect on the expression of low molecular weight cytokeratins or human leukocyte class I antigens, suggesting that GATA2 does not mediate its biological effects through phenotypic modulation of the T-IC pool. Moreover, our gene expression analysis indicated that GATA2 does not regulate the Notch and Hedgehog signaling pathways (Figures 3A and 3B). To investigate the reciprocal hypothesis, we used RNA interference to knock down NOTCH2 and SMO in the chemotherapy-resistant cultures (Figure S7E). We observed that NOTCH2 knockdown reduced the mRNA levels of HES1 (Figure S7E) and GATA2 (Figure 7A), while SMO knockdown reduced the mRNA levels of GLI1 and GLI2 (Figure S7E) but not GATA2 (Figure S7F). Interestingly, a recent report found that AKT regulates the mRNA and protein levels of GATA2 (Wang et al., 2012). In conjunction with our previous finding that NOTCH2 regulates AKT activation in our models, this report led us to speculate that Notch signaling may regulate GATA2 expression through AKT. Indeed, NOTCH2 knockdown reduced the activation of AKT as well as the protein levels of GATA2 (Figure 7B). Moreover, myristoylated AKT (myrAKT) increased the mRNA (Figure 7C) and protein (Figure 7D) levels of GATA2 in parental cells, while the AKT inhibitor MK2206 reduced them in chemotherapy-resistant cells (Figures 7E and 7F). Therefore, our models exhibited crosstalk between Notch signaling and GATA2 through AKT. In addition, our data support a positive feedback loop whereby activated AKT partially regulates GATA2 expression.

Dual IGF1R/INSR Inhibition Restores the Efficacy of Chemotherapy and Improves Survival in Preclinical Models

Having implicated a GATA2-IGF2 axis in the aggressiveness of lethal prostate cancer, we next examined it for possible therapeutic opportunities (Figure 7G). We studied dual inhibitors of IGF1R and INSR because these kinases operate at the apex of the signaling axis and agents are currently in advanced clinical development. In particular, we focused on OSI-906, a potent, selective, and orally bioavailable dual IGF1R/INSR inhibitor, which is currently in a phase III trial for refractory adrenocortical carcinoma (Mulvihill et al., 2009).

We performed colony-formation, immunoblot, and flow cytometry experiments with the chemotherapy-resistant cultures in vitro. Monotherapy with OSI-906 or two other well-characterized dual IGF1R/INSR inhibitors exhibited negligible activity, while the inhibitors potently sensitized the three chemotherapy-resistant cultures to both docetaxel and cabazitaxel (Figures 8A, S8A, and S8B). For in vivo studies, we established subcutaneous tumors using the patient-derived LPC models as well as the xenograft-derived (Sramkoski et al., 1999) 22Rv1-DR culture. Consistent with our in vitro data and an ongoing phase II clinical trial (ClinicalTrials.gov, NCT01533246), OSI-906 exhibited modest activity as a single agent (Figure S8C). This observation suggested that insulin-like growth factor signaling inhibition alone is insufficient to significantly constrain the growth of established CRPC tumors in vivo. In contrast, OSI-906 strongly restored the efficacy of both docetaxel and cabazitaxel, as evidenced by tumor volume, weight, and cleaved caspase expression following 4 weeks of combination therapy (Figures 8B, 8C, and S8D). Moreover, pharmacodynamic studies confirmed that OSI-906 reduced phosphorylation of the IGF1R and INSR tyrosine kinases in these studies (Figure S8E).

To extend the therapeutic benefit of combination therapy to preclinical models of disseminated chemotherapy-resistant disease, we performed intracardiac (IC) injections of 22Rv1-DR, LPC1, and LPC2 cells as well as toxicity profiles and survival analyses. Similar to a previous report (Drake et al., 2005), IC injection of 22Rv1-DR cells resulted in metastatic colonization of bone, liver, and other organs, recapitulating disseminated human disease in vivo (data not shown). In the LPC models, we observed metastatic colonization of bone, liver, and, less frequently, other organs (Figure S8F). We also exploited the in vitro nature of the 22Rv1-DR model to generate a luciferase-labeled subline suitable for in vivo bioluminescent imaging. Our studies showed that addition of OSI-906 to standard chemotherapy confers therapeutic benefit, as evidenced by reduced photon flux in 22Rv1-DR (Figure 8D) and improved overall survival in all three independent preclinical models (Figure 8E). Notably, combining OSI-906 with weekly taxane chemotherapy

(C) Immunoblots of relevant insulin-like growth factor signaling protein levels in DU145-DR, 22Rv1-DR, and ARCaPM-DR cells stably expressing indicated control or GATA2 shRNAs as well as a control or IGF2 expression vector in serum-free conditions.

(D) Representative colony formations and quantifications of DU145-DR, 22Rv1-DR, and ARCaPM-DR cells following 72 hr treatment with PI3K/AKT (LY294002, 10 μM), JNK (SP00125, 10 μM), and MEK/ERK (U0126, 1 μM) pathway inhibitors alone or in combination with DMSO, docetaxel (125 nM), or cabazitaxel (DU145-DR and 22Rv1-DR, 25 nM; ARCaPM-DR, 5 nM). Scale bar, 100 μm. Data represent the mean ± SD. *$p < 0.05$.

(E) Representative soft agar colony-formation assays and quantifications of DU145-DR, 22Rv1-DR, and ARCaPM-DR cells treated continuously with the pathway inhibitor conditions described in (D). Scale bar, 100 μm. Data represent the mean ± SD. *$p < 0.05$.

See also Figure S6.

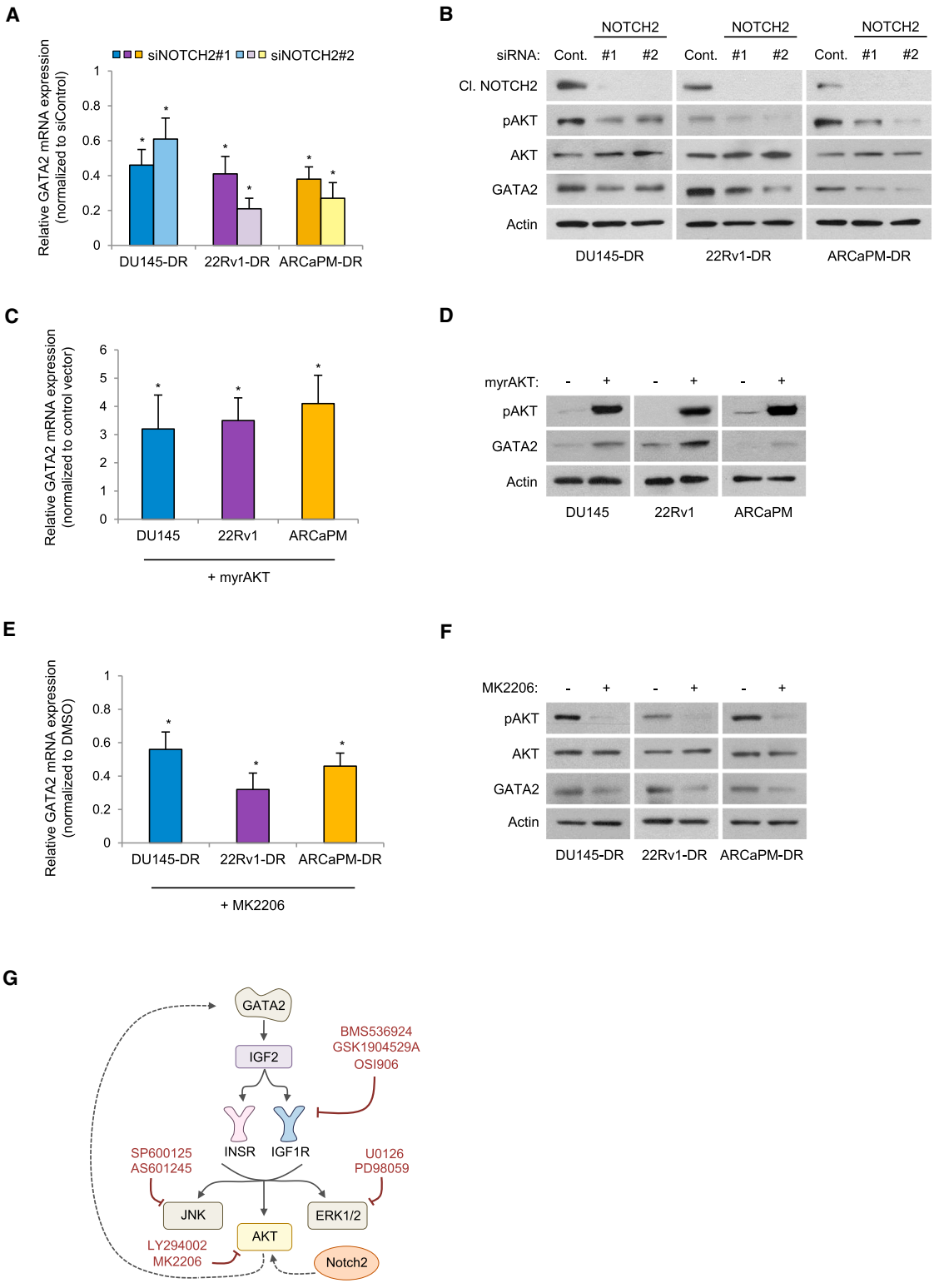

Figure 7. NOTCH2 Regulates GATA2 Expression through AKT Activation

(A) qRT-PCR of GATA2 mRNA levels in DU145-DR, 22Rv1-DR, and ARCaPM-DR cells transfected with control or NOTCH2 siRNAs. Data represent the mean ± SD. *$p < 0.05$.

(B) Immunoblots of indicated protein levels in cells from (A).

(C) qRT-PCR of GATA2 mRNA levels in DU145, 22Rv1, and ARCaPM cells stably expressing a control or myrAKT vector. Data represent the mean ± SD. *$p < 0.05$.

(legend continued on next page)

did not instigate a significant increase in general drug toxicity (Figure S8G).

DISCUSSION

Lethal prostate cancer is a widespread disease that merits continued investigation. We used experimental models and clinical databases to identify GATA2 as a determinant of aggressiveness in this context. Mechanistically, IGF2 emerged as an effector of GATA2 and a compelling therapeutic target. These results have implications for cancer biology and clinical oncology.

GATA2 Confers Aggressiveness in Lethal Prostate Cancer

The role of GATA2 in malignancy has been characterized in leukemia and NSCLC. In leukemia, both loss-of-function and gain-of-function events promote tumorigenesis and progression (Hahn et al., 2011; Zhang et al., 2008). In contrast, our data from CRPC as well as a detailed study of NSCLC (Kumar et al., 2012) suggest that GATA2 deficiency is strongly detrimental to the development and progression of solid tumors. In NSCLC, GATA2 regulates the proteasome as well as IL1/NF-κB and RHO signaling (Kumar et al., 2012). Our studies in CRPC now suggest that GATA2 additionally regulates insulin-like growth factor signaling. Moreover, our studies both corroborate the dependency on GATA2 for in vivo growth in NSCLC (Kumar et al., 2012) and reveal a role in chemotherapy resistance. Therefore, our results suggest that GATA2 biology is both vital and heterogeneous in solid tumors.

In prostate cancer, GATA2 is an established pioneer factor for AR-regulated genes (Chen et al., 2013; Perez-Stable et al., 2000; Wang et al., 2007; Wu et al., 2014), although its functional significance, downstream effectors, and therapeutic merits have been unclear. Our studies reveal a GATA2 dependency of prostate cancer for both chemotherapy resistance and in vivo growth. Regarding the pioneer function of GATA2, our data from the AR-expressing 22Rv1-DR culture corroborate this role. In addition, functional and transcriptome studies from the AR-negative DU145-DR and ARCaPM-DR models revealed an unexpected AR-independent role for GATA2. Interestingly, this finding is consistent with a recent report conducted with the androgen-dependent LNCaP cell line, wherein the majority of genome-wide GATA2 binding sites did not overlap with those of AR (Wu et al., 2014). Moreover, we found that GATA2 regulates a core subset of clinically and biologically validated genes that comprise a rich molecular network of aggressiveness in prostate cancer. Through a focused genetic screen, we both confirmed the significance of known prostate cancer-progression-associated genes and identified others without previously well-characterized roles in this disease. Finally, our data from clinical data sets and paraffin-embedded tissues suggest that GATA2 may play additional roles in metastatic progression and castration resistance. Intriguingly, recent reports that GATA2 regulates cellular motility (Chiang et al., 2014) as well as the AR-dependent cell cycle gene UBE2C (Wang et al., 2009) suggest that these associations merit further investigation. Therefore, our results endorse an increasingly central and complex role for GATA2 in prostate cancer biology.

IGF2 Is an Effector of GATA2 and a Therapeutic Target

IGF2 regulated chemotherapy resistance and tumorigenicity downstream of GATA2 in our models, and IGF2 expression increased during prostate cancer progression in clinical databases. Further studies showed that IGF2 regulates the survival properties of CRPC cells, a finding consistent with a large literature supporting the association between insulin-like growth factor signaling and these properties (Vincent and Feldman, 2002). The survival functions of IGF2 were further credentialed by the finding that IGF2 activates a network of canonical kinases. Indeed, AKT and ERK are widely characterized regulators of cancer cell survival, and JNK signaling may also regulate this property (Vivas-Mejia et al., 2010; Yang et al., 2003). It is important to note, however, that the regulation of AKT by IGF2 may be reduced in the setting of PTEN inactivation, a frequent event in prostate cancer (Grasso et al., 2012; Taylor et al., 2010). Moreover, in prostate cancer, the PI3K/AKT and MAPK pathways are undoubtedly activated by a range of regulatory factors including, for example, the epidermal growth factor receptor family (Chen et al., 2011; Gan et al., 2010; Qiu et al., 1998).

Finally, IGF2 may bind to both the IGF1R and INSR tyrosine kinases, a property with significant therapeutic implications in the setting of IGF2 overexpression. Indeed, IGF2 was upregulated and signaled through both receptors in our models. These observations favored dual IGF1R/INSR inhibition as the most promising therapeutic strategy, and in vitro as well as in vivo studies corroborated this approach. Interestingly, addition of an IGF1R antibody to docetaxel chemotherapy failed to confer therapeutic benefit in a recent phase II clinical trial that included patients with CRPC (de Bono et al., 2014). Our finding that IGF2 upregulation and INSR activation play key roles in insulin-like growth factor pathway signaling in CRPC predict that anti-IGF1R monotherapy is unlikely to be effective and, therefore, may provide an explanation for the results from this trial. The observation that IGF2 expression and INSR activation are robust mediators of IGF1R antibody resistance in laboratory models further supports this hypothesis (Buck et al., 2010). Therefore, in addition to their biological merits, our results provide a framework to both interpret previous clinical studies as well as design future trials with a more complete understanding of the relevant molecular pathophysiology.

(D) Immunoblots of indicated protein levels in cells from (C).

(E) qRT-PCR of GATA2 mRNA levels in DU145-DR, 22Rv1-DR, and ARCaPM-DR cells following 72 hr treatment with DMSO or the AKT inhibitor MK2206 (1 μM). Data represent the mean ± SD. *$p < 0.05$.

(F) Immunoblots of indicated protein levels in cells from (E).

(G) Schematic representation of the polykinase program activated by the GATA2-IGF2 axis, crosstalk with NOTCH2, and possible therapeutic opportunities. See also Figure S7.

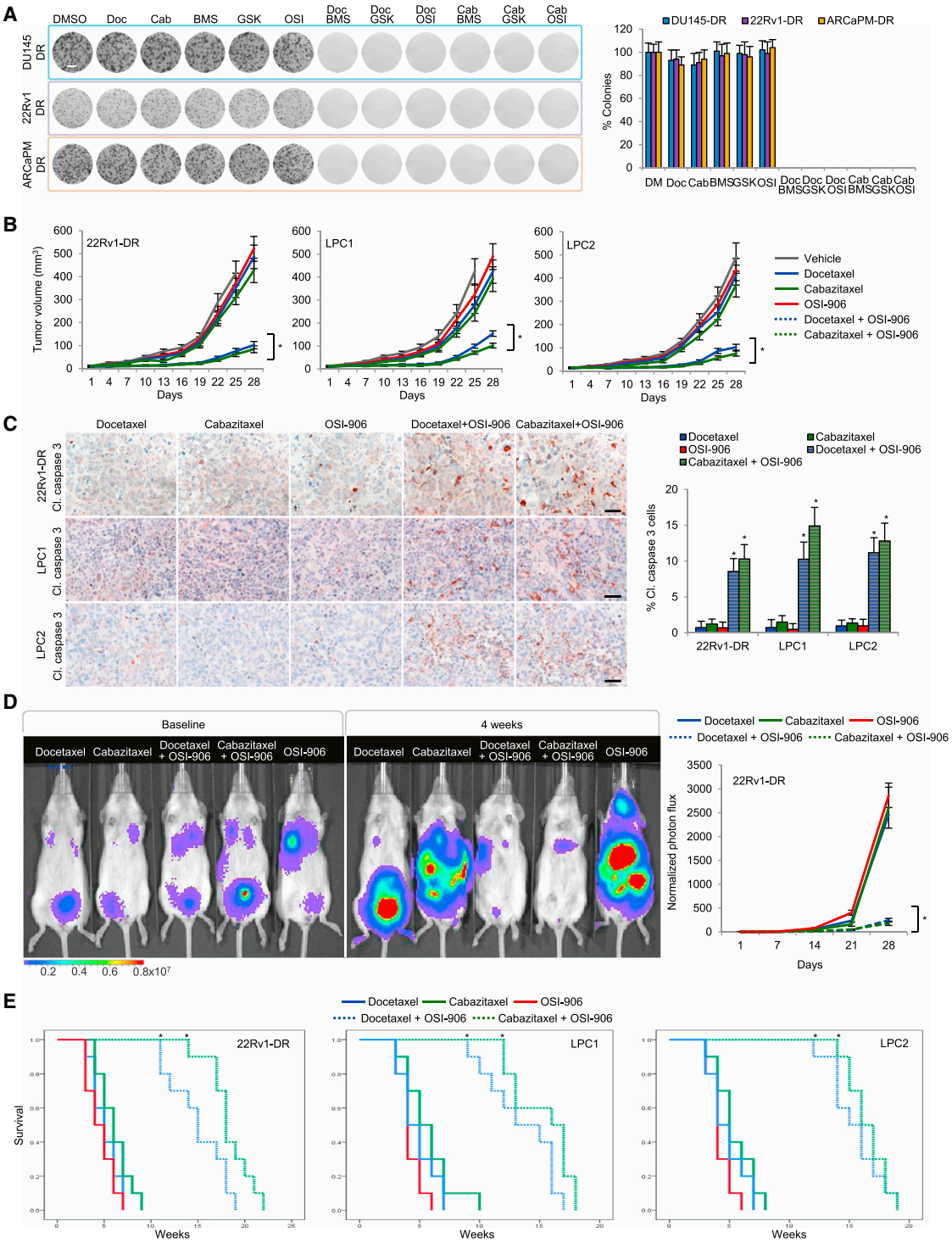

Figure 8. Dual IGF1R/INSR Inhibition Improves the Efficacy of Chemotherapy and Survival in Preclinical Models of Lethal Prostate Cancer

(A) Representative colony-formation assays and quantifications of DU145-DR, 22Rv1-DR, and ARCaPM-DR cells following 72 hr treatment with DMSO, docetaxel (125 nM), or cabazitaxel (DU145-DR and 22Rv1-DR, 25 nM; ARCaPM-DR, 5 nM) as well as the dual IGF1R/INSR inhibitors BMS-536924 (1 μM), GSK-1904529A (1 μM), and OSI-906 (1 μM) or vehicle control. Data represent the mean ± SD.

(B) Volumes of subcutaneous 22Rv1-DR, LPC1, and LPC2 xenografts during 28 days of combination therapy with vehicle, docetaxel (10 mg/kg i.p. weekly), or cabazitaxel (10 mg/kg i.p. weekly) as well as OSI-906 (25 mg/kg orally 4 days weekly) or vehicle control. Data represent the mean ± SD. *$p < 0.05$.

(C) Representative immunohistochemistry images and quantifications of cleaved caspase 3 levels in subcutaneous 22Rv1-DR, LPC1, and LPC2 xenografts after 14 days of the combination therapy described in (B). Scale bar, 100 μm. Data represent the mean ± SD. *$p < 0.05$.

(legend continued on next page)

EXPERIMENTAL PROCEDURES

Docetaxel-Resistant Prostate Cancer Cell Models

The sublines DU145-DR and 22Rv1-DR were described previously (Domingo-Domenech et al., 2012). ARCaPM cells were obtained and maintained in prostate epithelial cell medium (both Novicure Biotechnology) supplemented with 10% fetal bovine serum. Cells were grown at 37°C in a humidified atmosphere with 5% CO_2. Resistant clones were selected by culturing cells with docetaxel dissolved in DMSO for 72 hr. A dose-escalation strategy was implemented for 7 months until a concentration of 1 μM was reached. In parallel, parental ARCaPM cells were exposed to equal volumes of DMSO.

Human Paraffin-Embedded Prostate Cancer Tissues

Human formalin-fixed paraffin-embedded primary (n = 56), metastatic CRPC (n = 35), and taxane-treated metastatic CRPC (n = 33) tissue samples were collected from the Mount Sinai Medical Center tumor biorepository under an Institutional Review Board-approved protocol, and informed consent was obtained from all subjects. All tissue sections were reviewed by a pathologist to confirm prostate cancer origin.

In Vivo siRNA Knockdown

All protocols for mouse experiments were in accordance with institutional guidelines and were approved by the Mount Sinai Medical Center Institutional Animal Care and Use Committee. Two GATA2-targeting siRNA clones (s5596 and s5598), two IGF2-targeting siRNA clones (s7214 and s7215), and a non-targeting control (all Life Technologies) were selected on the basis of their activity in the chemotherapy-resistant cultures in vitro. High-performance liquid chromatography-purified in vivo-ready siRNAs were diluted to a stock concentration of 3 mg/ml before being combined with complexation buffer and Invivofectamine (both Invitrogen), in accordance with the manufacturer's instructions. The resulting solution was dialyzed in 1 l of 1× PBS for 1 hr using 8–10 kDa Float-A-Lyzer devices (Spectrum Laboratories), in accordance with the manufacturer's instructions. The dialyzed solutions were stored at 4°C for up to 2 weeks. For intratumoral administration, palpable tumors were shaved and slowly injected with dialyzed siRNA solutions at a concentration of 50 μg/100 mm^3 using 30.5 guage needles twice weekly.

In Vivo Bioluminescence Imaging

Imaging was performed using an IVIS Spectrum imager (Xenogen). Animals were anesthetized using an isoflurane vaporizer and placed onto the warmed stage inside the camera box. Animals next received intraperitoneal luciferin (200 mg/kg) 5 min prior to imaging. For quantification, rectangular regions of interest incorporating the entire animal were measured. The signal was measured in photons per second using Living Image software.

Statistical Analyses

Statistical analysis was carried out with SPSS software unless otherwise specified. Experimental data expressed as mean ± SD were analyzed by Student's t test. All t tests were conducted at the two-sided 0.05 level of significance. For genomic analyses, multiple testing significance was calculated using Significance Analysis of Microarrays or Tuxedo software. For preclinical studies, survival analyses were performed using the Kaplan-Meier method and curves were compared by the log rank test.

ACCESSION NUMBERS

The Gene Expression Omnibus accession number for the RNA sequencing data reported in this manuscript is GSE58966.

SUPPLEMENTAL INFORMATION

Supplemental Information includes Supplemental Experimental Procedures and eight figures and can be found with this article online at http://dx.doi.org/10.1016/j.ccell.2014.11.013.

ACKNOWLEDGMENTS

We thank Dr. Yumi Kasai and Violeta Capric from the Genomics Core Facility in the Department of Genetics and Genomic Sciences at the Mount Sinai Medical Center for their assistance in performing the RNA sequencing of samples. We thank Dr. Jordi Orchando and Qiao Xuqiang from the Flow Cytometry Shared Resource at the Mount Sinai Medical Center for their assistance in flow cytometry analysis. We thank Dr. Rumana Huq and Lauren Orourke from the Microscopy Shared Resource Facility at the Mount Sinai Medical Center for their imaging assistance. We thank Dr.Yu Zhou of the In-vivo Molecular Imaging Shared Resource Facility at the Mount Sinai Medical Center for his assistance with mouse imaging experiments. We thank the Dr. Josep Maria Llovet laboratory at the Mount Sinai Medical Center for sharing reagents. We thank Dr. Ruth Kornreich from the Department of Genetics and Genomic Sciences at the Mount Sinai Medical Center for performing the genetic fingerprinting analysis. We thank Drs. Eva Domingo-Domenech and Margarita Garcia from the Catalan Institute of Oncology for harvesting circulating tumor cells from advanced prostate cancer patients. Finally, we thank the TJ Martell Foundation for its support of this project.

Received: July 9, 2014
Revised: October 7, 2014
Accepted: November 13, 2014
Published: January 12, 2015

REFERENCES

Bates, P., Fisher, R., Ward, A., Richardson, L., Hill, D.J., and Graham, C.F. (1995). Mammary cancer in transgenic mice expressing insulin-like growth factor II (IGF-II). Br. J. Cancer *72*, 1189–1193.

Beer, T.M., Armstrong, A.J., Rathkopf, D.E., Loriot, Y., Sternberg, C.N., Higano, C.S., Iversen, P., Bhattacharya, S., Carles, J., Chowdhury, S., et al. (2014). Enzalutamide in metastatic prostate cancer before chemotherapy. N. Engl. J. Med. *371*, 424–433.

Bishr, M., and Saad, F. (2013). Overview of the latest treatments for castration-resistant prostate cancer. Nat. Rev. Urol. *10*, 522–528.

Buck, E., Gokhale, P.C., Koujak, S., Brown, E., Eyzaguirre, A., Tao, N., Rosenfeld-Franklin, M., Lerner, L., Chiu, M.I., Wild, R., et al. (2010). Compensatory insulin receptor (IR) activation on inhibition of insulin-like growth factor-1 receptor (IGF-1R): rationale for cotargeting IGF-1R and IR in cancer. Mol. Cancer Ther. *9*, 2652–2664.

Chen, L., Mooso, B.A., Jathal, M.K., Madhav, A., Johnson, S.D., van Spyk, E., Mikhailova, M., Zierenberg-Ripoll, A., Xue, L., Vinall, R.L., et al. (2011). Dual EGFR/HER2 inhibition sensitizes prostate cancer cells to androgen withdrawal by suppressing ErbB3. Clin. Cancer Res. *17*, 6218–6228.

Chen, Y., Chi, P., Rockowitz, S., Iaquinta, P.J., Shamu, T., Shukla, S., Gao, D., Sirota, I., Carver, B.S., Wongvipat, J., et al. (2013). ETS factors reprogram the androgen receptor cistrome and prime prostate tumorigenesis in response to PTEN loss. Nat. Med. *19*, 1023–1029.

Chiang, Y.T., Wang, K., Fazli, L., Qi, R.Z., Gleave, M.E., Collins, C.C., Gout, P.W., and Wang, Y. (2014). GATA2 as a potential metastasis-driving gene in prostate cancer. Oncotarget *5*, 451–461.

(D) Bioluminescence of IC-administered 22Rv1-DR luciferase-expressing cells during 28 days of the combination therapy described in (B). Data represent the mean ± SD. *$p < 0.05$.
(E) Kaplan-Meier survival analysis following IC administration of 22Rv1-DR, LPC1, and LPC2 cells and the combination therapy described (B). *$p < 0.05$.
See also Figure S8.

Christofori, G., Naik, P., and Hanahan, D. (1994). A second signal supplied by insulin-like growth factor II in oncogene-induced tumorigenesis. Nature *369*, 414–418.

Church, D.N., Phillips, B.R., Stuckey, D.J., Barnes, D.J., Buffa, F.M., Manek, S., Clarke, K., Harris, A.L., Carter, E.J., and Hassan, A.B. (2012). Igf2 ligand dependency of Pten(+/-) developmental and tumour phenotypes in the mouse. Oncogene *31*, 3635–3646.

de Bono, J.S., Oudard, S., Ozguroglu, M., Hansen, S., Machiels, J.P., Kocak, I., Gravis, G., Bodrogi, I., Mackenzie, M.J., Shen, L., et al.; TROPIC Investigators (2010). Prednisone plus cabazitaxel or mitoxantrone for metastatic castration-resistant prostate cancer progressing after docetaxel treatment: a randomised open-label trial. Lancet *376*, 1147–1154.

de Bono, J.S., Logothetis, C.J., Molina, A., Fizazi, K., North, S., Chu, L., Chi, K.N., Jones, R.J., Goodman, O.B., Jr., Saad, F., et al.; COU-AA-301 Investigators (2011). Abiraterone and increased survival in metastatic prostate cancer. N. Engl. J. Med. *364*, 1995–2005.

de Bono, J.S., Piulats, J.M., Pandha, H.S., Petrylak, D.P., Saad, F., Aparicio, L.M., Sandhu, S.K., Fong, P., Gillessen, S., Hudes, G.R., et al. (2014). Phase II randomized study of figitumumab plus docetaxel and docetaxel alone with crossover for metastatic castration-resistant prostate cancer. Clin. Cancer Res. *20*, 1925–1934.

Domingo-Domenech, J., Vidal, S.J., Rodriguez-Bravo, V., Castillo-Martin, M., Quinn, S.A., Rodriguez-Barrueco, R., Bonal, D.M., Charytonowicz, E., Gladoun, N., de la Iglesia-Vicente, J., et al. (2012). Suppression of acquired docetaxel resistance in prostate cancer through depletion of notch- and hedgehog-dependent tumor-initiating cells. Cancer Cell *22*, 373–388.

Drake, J.M., Gabriel, C.L., and Henry, M.D. (2005). Assessing tumor growth and distribution in a model of prostate cancer metastasis using bioluminescence imaging. Clin. Exp. Metastasis *22*, 674–684.

Feinberg, A.P., and Tycko, B. (2004). The history of cancer epigenetics. Nat. Rev. Cancer *4*, 143–153.

Gan, Y., Shi, C., Inge, L., Hibner, M., Balducci, J., and Huang, Y. (2010). Differential roles of ERK and Akt pathways in regulation of EGFR-mediated signaling and motility in prostate cancer cells. Oncogene *29*, 4947–4958.

Grasso, C.S., Wu, Y.M., Robinson, D.R., Cao, X., Dhanasekaran, S.M., Khan, A.P., Quist, M.J., Jing, X., Lonigro, R.J., Brenner, J.C., et al. (2012). The mutational landscape of lethal castration-resistant prostate cancer. Nature *487*, 239–243.

Hahn, H., Wojnowski, L., Specht, K., Kappler, R., Calzada-Wack, J., Potter, D., Zimmer, A., Müller, U., Samson, E., Quintanilla-Martinez, L., and Zimmer, A. (2000). Patched target Igf2 is indispensable for the formation of medulloblastoma and rhabdomyosarcoma. J. Biol. Chem. *275*, 28341–28344.

Hahn, C.N., Chong, C.E., Carmichael, C.L., Wilkins, E.J., Brautigan, P.J., Li, X.C., Babic, M., Lin, M., Carmagnac, A., Lee, Y.K., et al. (2011). Heritable GATA2 mutations associated with familial myelodysplastic syndrome and acute myeloid leukemia. Nat. Genet. *43*, 1012–1017.

Jarrard, D.F., Bussemakers, M.J., Bova, G.S., and Isaacs, W.B. (1995). Regional loss of imprinting of the insulin-like growth factor II gene occurs in human prostate tissues. Clin. Cancer Res. *1*, 1471–1478.

Jemal, A., Bray, F., Center, M.M., Ferlay, J., Ward, E., and Forman, D. (2011). Global cancer statistics. CA Cancer J. Clin. *61*, 69–90.

Kumar, M.S., Hancock, D.C., Molina-Arcas, M., Steckel, M., East, P., Diefenbacher, M., Armenteros-Monterroso, E., Lassailly, F., Matthews, N., Nye, E., et al. (2012). The GATA2 transcriptional network is requisite for RAS oncogene-driven non-small cell lung cancer. Cell *149*, 642–655.

Liu, R., Wang, X., Chen, G.Y., Dalerba, P., Gurney, A., Hoey, T., Sherlock, G., Lewicki, J., Shedden, K., and Clarke, M.F. (2007). The prognostic role of a gene signature from tumorigenic breast-cancer cells. N. Engl. J. Med. *356*, 217–226.

Livingstone, C. (2013). IGF2 and cancer. Endocr. Relat. Cancer *20*, R321–R339.

Lubik, A.A., Gunter, J.H., Hollier, B.G., Ettinger, S., Fazli, L., Stylianou, N., Hendy, S.C., Adomat, H.H., Gleave, M.E., Pollak, M., et al. (2013). IGF2 increases de novo steroidogenesis in prostate cancer cells. Endocr. Relat. Cancer *20*, 173–186.

Lui, J.C., and Baron, J. (2013). Evidence that Igf2 down-regulation in postnatal tissues and up-regulation in malignancies is driven by transcription factor E2f3. Proc. Natl. Acad. Sci. USA *110*, 6181–6186.

Moorehead, R.A., Sanchez, O.H., Baldwin, R.M., and Khokha, R. (2003). Transgenic overexpression of IGF-II induces spontaneous lung tumors: a model for human lung adenocarcinoma. Oncogene *22*, 853–857.

Mulvihill, M.J., Cooke, A., Rosenfeld-Franklin, M., Buck, E., Foreman, K., Landfair, D., O'Connor, M., Pirritt, C., Sun, Y., Yao, Y., et al. (2009). Discovery of OSI-906: a selective and orally efficacious dual inhibitor of the IGF-1 receptor and insulin receptor. Future Med. Chem. *1*, 1153–1171.

Perez-Stable, C.M., Pozas, A., and Roos, B.A. (2000). A role for GATA transcription factors in the androgen regulation of the prostate-specific antigen gene enhancer. Mol. Cell. Endocrinol. *167*, 43–53.

Petrylak, D.P., Tangen, C.M., Hussain, M.H., Lara, P.N., Jr., Jones, J.A., Taplin, M.E., Burch, P.A., Berry, D., Moinpour, C., Kohli, M., et al. (2004). Docetaxel and estramustine compared with mitoxantrone and prednisone for advanced refractory prostate cancer. N. Engl. J. Med. *351*, 1513–1520.

Pravtcheva, D.D., and Wise, T.L. (1998). Metastasizing mammary carcinomas in H19 enhancers-Igf2 transgenic mice. J. Exp. Zool. *281*, 43–57.

Qiu, Y., Ravi, L., and Kung, H.J. (1998). Requirement of ErbB2 for signalling by interleukin-6 in prostate carcinoma cells. Nature *393*, 83–85.

Rogler, C.E., Yang, D., Rossetti, L., Donohoe, J., Alt, E., Chang, C.J., Rosenfeld, R., Neely, K., and Hintz, R. (1994). Altered body composition and increased frequency of diverse malignancies in insulin-like growth factor-II transgenic mice. J. Biol. Chem. *269*, 13779–13784.

Ryan, C.J., Smith, M.R., de Bono, J.S., Molina, A., Logothetis, C.J., de Souza, P., Fizazi, K., Mainwaring, P., Piulats, J.M., Ng, S., et al.; COU-AA-302 Investigators (2013). Abiraterone in metastatic prostate cancer without previous chemotherapy. N. Engl. J. Med. *368*, 138–148.

Scher, H.I., Fizazi, K., Saad, F., Taplin, M.E., Sternberg, C.N., Miller, K., de Wit, R., Mulders, P., Chi, K.N., Shore, N.D., et al.; AFFIRM Investigators (2012). Increased survival with enzalutamide in prostate cancer after chemotherapy. N. Engl. J. Med. *367*, 1187–1197.

Sharma, N.L., Massie, C.E., Ramos-Montoya, A., Zecchini, V., Scott, H.E., Lamb, A.D., MacArthur, S., Stark, R., Warren, A.Y., Mills, I.G., and Neal, D.E. (2013). The androgen receptor induces a distinct transcriptional program in castration-resistant prostate cancer in man. Cancer Cell *23*, 35–47.

Sramkoski, R.M., Pretlow, T.G., 2nd, Giaconia, J.M., Pretlow, T.P., Schwartz, S., Sy, M.S., Marengo, S.R., Rhim, J.S., Zhang, D., and Jacobberger, J.W. (1999). A new human prostate carcinoma cell line, 22Rv1. In Vitro Cell. Dev. Biol. Anim. *35*, 403–409.

Stylianopoulou, F., Efstratiadis, A., Herbert, J., and Pintar, J. (1988). Pattern of the insulin-like growth factor II gene expression during rat embryogenesis. Development *103*, 497–506.

Tada, Y., Yamaguchi, Y., Kinjo, T., Song, X., Akagi, T., Takamura, H., Ohta, T., Yokota, T., and Koide, H. (2014). The stem cell transcription factor ZFP57 induces IGF2 expression to promote anchorage-independent growth in cancer cells. Oncogene.

Tannock, I.F., de Wit, R., Berry, W.R., Horti, J., Pluzanska, A., Chi, K.N., Oudard, S., Théodore, C., James, N.D., Turesson, I., et al.; TAX 327 Investigators (2004). Docetaxel plus prednisone or mitoxantrone plus prednisone for advanced prostate cancer. N. Engl. J. Med. *351*, 1502–1512.

Taylor, B.S., Schultz, N., Hieronymus, H., Gopalan, A., Xiao, Y., Carver, B.S., Arora, V.K., Kaushik, P., Cerami, E., Reva, B., et al. (2010). Integrative genomic profiling of human prostate cancer. Cancer Cell *18*, 11–22.

Vicente, C., Conchillo, A., García-Sánchez, M.A., and Odero, M.D. (2012a). The role of the GATA2 transcription factor in normal and malignant hematopoiesis. Crit. Rev. Oncol. Hematol. *82*, 1–17.

Vicente, C., Vazquez, I., Conchillo, A., García-Sánchez, M.A., Marcotegui, N., Fuster, O., González, M., Calasanz, M.J., Lahortiga, I., and Odero, M.D. (2012b). Overexpression of GATA2 predicts an adverse prognosis for patients with acute myeloid leukemia and it is associated with distinct molecular abnormalities. Leukemia *26*, 550–554.

Vincent, A.M., and Feldman, E.L. (2002). Control of cell survival by IGF signaling pathways. Growth Horm. IGF Res. *12*, 193–197.

Vivas-Mejia, P., Benito, J.M., Fernandez, A., Han, H.D., Mangala, L., Rodriguez-Aguayo, C., Chavez-Reyes, A., Lin, Y.G., Carey, M.S., Nick, A.M., et al. (2010). c-Jun-NH2-kinase-1 inhibition leads to antitumor activity in ovarian cancer. Clin. Cancer Res. *16*, 184–194.

Wang, Q., Li, W., Liu, X.S., Carroll, J.S., Jänne, O.A., Keeton, E.K., Chinnaiyan, A.M., Pienta, K.J., and Brown, M. (2007). A hierarchical network of transcription factors governs androgen receptor-dependent prostate cancer growth. Mol. Cell *27*, 380–392.

Wang, Q., Li, W., Zhang, Y., Yuan, X., Xu, K., Yu, J., Chen, Z., Beroukhim, R., Wang, H., Lupien, M., et al. (2009). Androgen receptor regulates a distinct transcription program in androgen-independent prostate cancer. Cell *138*, 245–256.

Wang, Y., He, X., Ngeow, J., and Eng, C. (2012). GATA2 negatively regulates PTEN by preventing nuclear translocation of androgen receptor and by androgen-independent suppression of PTEN transcription in breast cancer. Hum. Mol. Genet. *21*, 569–576.

Wu, D., Sunkel, B., Chen, Z., Liu, X., Ye, Z., Li, Q., Grenade, C., Ke, J., Zhang, C., Chen, H., et al. (2014). Three-tiered role of the pioneer factor GATA2 in promoting androgen-dependent gene expression in prostate cancer. Nucleic Acids Res. *42*, 3607–3622.

Yang, Y.M., Bost, F., Charbono, W., Dean, N., McKay, R., Rhim, J.S., Depatie, C., and Mercola, D. (2003). C-Jun NH(2)-terminal kinase mediates proliferation and tumor growth of human prostate carcinoma. Clin. Cancer Res. *9*, 391–401.

Zhang, S.J., Ma, L.Y., Huang, Q.H., Li, G., Gu, B.W., Gao, X.D., Shi, J.Y., Wang, Y.Y., Gao, L., Cai, X., et al. (2008). Gain-of-function mutation of GATA-2 in acute myeloid transformation of chronic myeloid leukemia. Proc. Natl. Acad. Sci. USA *105*, 2076–2081.